

439 Supporting Material (SM): Contact, travel, &
 440 transmission

441 **Contents**

442 **S1 Medical claims data** **20**

443 S1.1 Definition of ILI incidence ratio 20

444 S1.2 Zip3 ILI incidence ratio during the holidays 21

445 S1.3 Estimation of the effective reproductive number 21

446 S1.4 Verifying flu activity during the holidays 22

447 **S2 Metapopulation model** **23**

448 S2.1 Demographic and contact data 23

449 S2.1.1 Age-specific contact matrix 24

450 S2.2 Travel data 26

451 S2.3 Holiday intervention period 26

452 S2.4 Comparison of baseline and holiday air travel networks 27

453 **S3 Sensitivity Analysis of Model Results** **28**

454 S3.1 Contribution of contact reduction vs. assortativity to holiday changes 28

455 S3.2 Sensitivity of epidemic outcomes to contact reduction 29

456 S3.3 Sensitivity of epidemic outcomes to holiday timing 29

457 S3.4 Data access 33

458 **S1 Medical claims data**

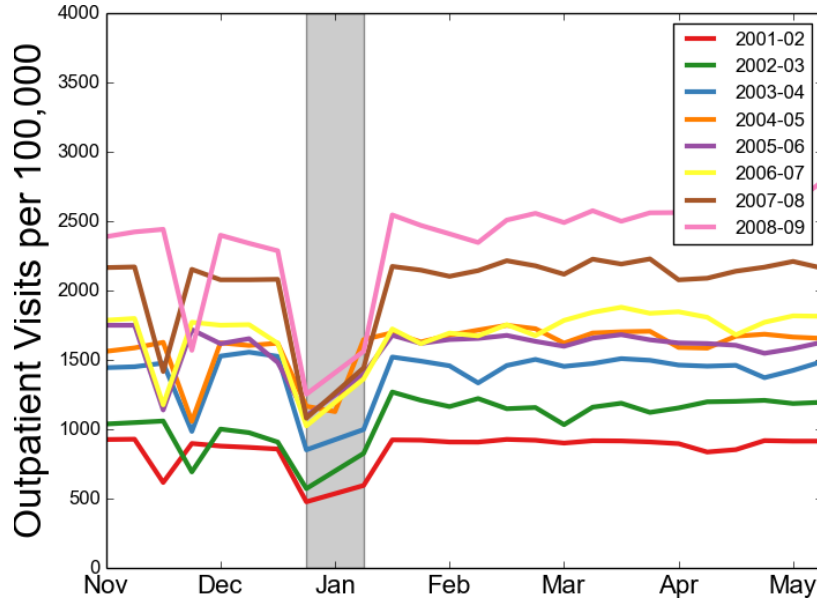
459 **S1.1 Definition of ILI incidence ratio**

460 We use the ILI incidence ratio as defined in [32]. Parameters referenced in the equation are described
 461 in Table S1.

$$\rho_{w,s} = (d_{w,s}/v_{w,s}) \times (p_s/100,000) \tag{1}$$

462 The incorporation of visits into this metric helps to account for artificialities in the medical claims
463 data related to to physician office closures and changes to care-seeking behavior during the holidays,
464 and increasing database coverage over time (Figure S1).

Figure S1: **Total visits to physicians reported by the medical claims dataset drops during holiday periods.** The grey bar highlights the typical school holiday for winter break, and a short dip (not highlighted) in late November demonstrates a similar pattern during the Thanksgiving holiday. Coverage in the medical claims dataset increases over time, as witnessed by the rising visit rates in each flu season.



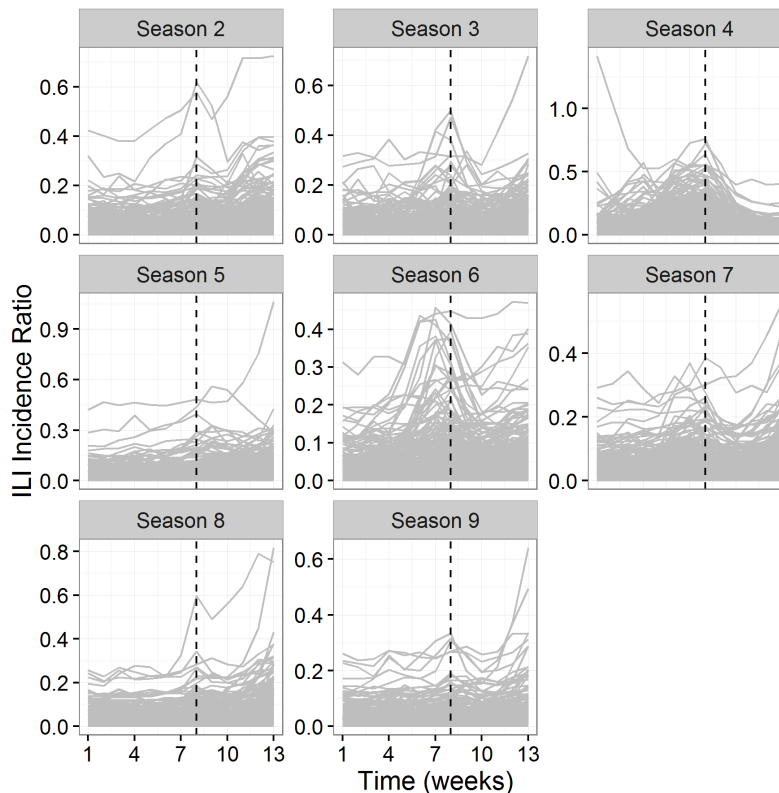
465 S1.2 Zip3 ILI incidence ratio during the holidays

466 We observed holiday-associated dips in the ILI incidence ratio at the zip3-level for each season
467 (Figure S2).

468 S1.3 Estimation of the effective reproductive number

469 To understand the effect of the winter holidays on flu transmission in the empirical data, we estimated
470 the effective reproductive number (R_t), the average number of secondary cases generated by each
471 infected individual under the conditions at time t , over weekly periods during the eight flu seasons
472 from 2001-2002 through 2008-2009. We used an estimated serial interval for flu of 3.6 days with
473 a standard deviation of 1.6 days [55]. These analyses were performed with the EpiEstim package
474 version 1.1-2 developed for the R programming language (R Foundation for Statistical Computing,
475 Vienna, Austria) [56]. The EpiEstim data inputs were the U.S. weekly ILI medical claims, adjusted in
476 two ways: 1) scaled up according to a ratio of total visits during a winter reference week to total visits

Figure S2: **ILI incidence ratio during the holiday period for each study season at the zip3-level.** Each grey line represents the time series for a single zip3, and the dashed line indicates the week including Christmas.



477 during the reporting week, in order to account for temporal changes in healthcare-seeking behavior,
 478 and 2) scaled up according to estimates that only 45% of the total population symptomatic with
 479 ILI seeks care from a physician (See SM section S1.3) [57, 58].

480 To account for changes in health care seeking behavior during holiday periods (Figure S1) and
 481 changes to medical claims coverage over time, we adjusted the raw ILI medical claims data for input
 482 into the EpiEstim program for estimation of the effective reproductive number R_t . Parameters
 483 referenced in the equation are described in Table S1.

$$d_{t,s}^* = (d_{w,s}/C) \times (v_{w_s}/v_{w,s}) \times (1/\phi) \quad (2)$$

484 S1.4 Verifying flu activity during the holidays

485 To examine whether ILI activity was due to influenza during the U.S. Thanksgiving and Christ-
 486 mas holidays, we used data that is publicly available from CDC's FluView Interactive application.

Table S1: **Parameters in adjustments to ILI medical claims data** The same notation was used to describe the ILI incidence ratio and the adjustments for the effective reproductive number analysis.

Common terms	
$d_{w,s}$	raw ILI cases at week w in season s
$v_{w,s}$	total visits to health care facilities for any diagnosis at week w in season s
Specific to equation 1	
$\rho_{w,s}$	ILI incidence ratio (IR) at week w in season s
p_s	population size in season s
Specific to equation 2	
$d_{t,s}^*$	adjusted ILI cases at day t in season s , input for effective reproductive number analysis
v_{w_s}	total visits to health care facilities for any diagnosis at winter reference week w_s
ϕ	estimate of the proportion of the total population that seeks care for symptomatic influenza-like illness (0.45)
Indicator variables	
w_s	winter reference week (chosen as the week of November 1 in a given season s)
t	indicator for time in days
s	indicator for flu season
w	indicator for time in weeks
C	number of days in a week (7 days)

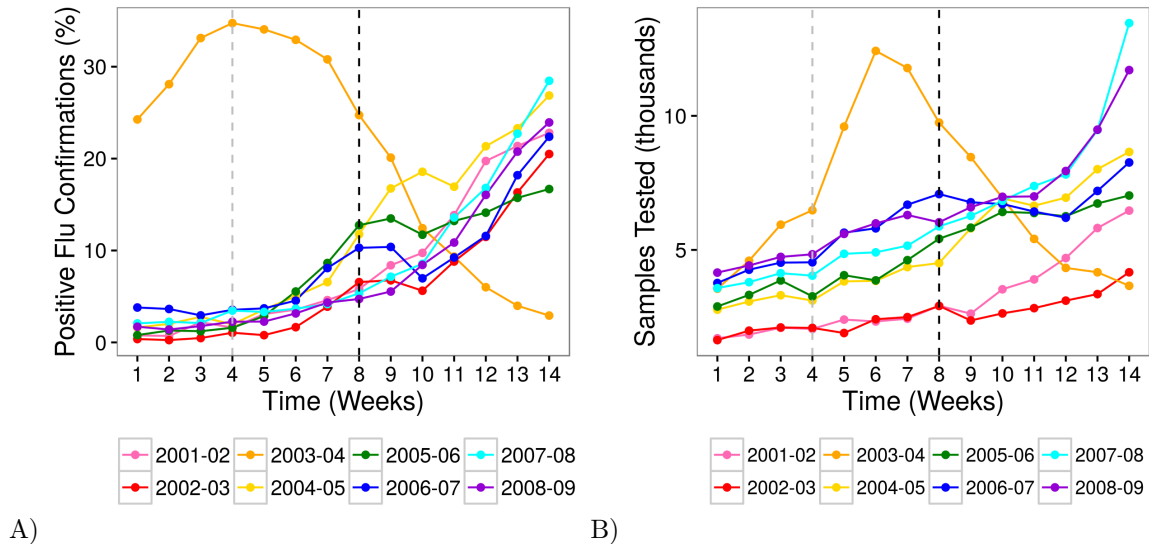
487 These data were collected by the WHO/NREVSS Collaborating Labs and they represent the per-
 488 centage of influenza-positive laboratory confirmations among all tested respiratory specimens in this
 489 CDC influenza surveillance system. We found that flu was regularly circulating by Christmas, but
 490 largely absent during the earlier Thanksgiving holidays (Figure S3A). During both holiday periods,
 491 thousands of samples were tested for influenza (Figure S3B).

492 S2 Metapopulation model

493 S2.1 Demographic and contact data

494 Spatial areas were modeled after metropolitan areas (236 areas were included, covering 79% of the
 495 U.S. population) as defined by the U.S. Bureau of Transportation Statistics. Each metropolitan
 496 area's population was divided into children (24%) and adults (76%), according to the national age
 497 distribution reported in the 2010 U.S. Census. Age-specific contact rates were adapted from a contact
 498 survey from Germany, given the similarity in demography to the United States [7], and translated
 499 to a contact matrix between children and adults (See SM section S2.1.1). Transmission parameters
 500 were chosen so that final epidemic sizes were 15-20% of the population [59], and the recovery rate

Figure S3: **Flu activity is typically present during the Christmas holiday, but largely absent during the Thanksgiving holiday.** A) The percentage of influenza-positive laboratory confirmations over time, as collected from WHO/NREVSS, from the first week in November to the last week in January for flu seasons from 2001 to 2009. B) The number of samples tested for flu from WHO/NREVSS during the holiday period. The black dashed line represents the week of Christmas, and the grey dashed line represents the week of Thanksgiving.



501 corresponded to a two day infectious period, according to epidemiological survey data [60].

502 S2.1.1 Age-specific contact matrix

503 We utilize the following contact matrix structure where C_{cc} is the average number of daily contacts
 504 between children and C_{ac} is the average number of daily adult contacts reported by children, etc.

$$\begin{pmatrix} C_{cc} & C_{ca} \\ C_{ac} & C_{aa} \end{pmatrix}$$

505 Of the countries included in the study by Mossong et al ([7]), Germany represents a population
 506 most similar to the United States. Thus, we calculated the average number of daily contacts from
 507 German contact data using the following matrix, where q_c is the average number of child daily
 508 contacts weighted by German child population size, q_a is the average number of adult daily contacts
 509 weighted by German adult population size, p_c is the fraction of child daily contacts that occur
 510 with other children, p_a is the fraction of adult daily contacts that occur with other adults [7]. The

511 parameter α is the fraction of the U.S. population represented by children [33].

$$\begin{pmatrix} p_c q_c / \alpha & (1 - p_a) q_a / \alpha \\ (1 - p_c) q_c / (1 - \alpha) & p_a q_a / (1 - \alpha) \end{pmatrix}$$

512 Age subgroups of children are indicated with subscript i (0-5, 10-14, and 15-19 years old), age
 513 subgroups of adults are indicated with subscript j (20-24, 25-29, 30-34, 35-39, 40-44, 45-49, 50-54,
 514 55-59, 60-64, 65-69 years old). The average number of child daily contacts q_c and adult daily contacts
 515 q_a were calculated, where $x_{i,l}$ is the number of daily contacts between age subgroup i and all ages
 516 l , g_i or g_j is the population size of the age subgroup, g_c is the total child population size, and g_a is
 517 the total adult population size, and the number of subgroups for children and adults are denoted by
 518 N_i and N_j , respectively.

$$q_c = \sum_{i=1}^{N_i} (x_{i,l} \times g_i) / (g_c) \quad (3)$$

$$q_a = \sum_{j=1}^{N_j} (x_{j,l} \times g_j) / (g_a) \quad (4)$$

519 The fraction of child daily contacts that occur with other children p_c and the fraction of adult
 520 daily contacts that occur with other adults p_a were calculated as the ratio of the average number of
 521 within group contacts $r_{c/a}$ to the average number of total contacts $q_{c/a}$.

$$p_c = r_c / q_c \quad (5)$$

$$p_a = r_a / q_a \quad (6)$$

522 The average number of daily contacts that children had with other children r_c and that adults
 523 had with other adults r_a was calculated, where $x_{i,c}$ is the average number of daily contacts of child
 524 subgroup i with children c , and $x_{i,a}$ is the average number of daily contacts of adult subgroup i with
 525 adults a .

$$r_c = \sum_{i=1}^{N_i} (x_{i,c} \times g_i) / (g_c) \quad (7)$$

$$r_a = \sum_{j=1}^{N_j} (x_{j,a} \times g_j) / (g_a) \quad (8)$$

526 Given this structure, we present three contact matrices used in multiple analyses, in order: the

527 non-holiday contact matrix, the full holiday contact matrix, and the partial contact matrix (SM
528 only).

$$\begin{pmatrix} 18.59 & 4.21 \\ 5.58 & 8.84 \end{pmatrix}$$

529

$$\begin{pmatrix} 7.78 & 2.55 \\ 5.83 & 8.15 \end{pmatrix}$$

530

$$\begin{pmatrix} 10.47 & 3.68 \\ 3.14 & 7.03 \end{pmatrix}$$

531 **S2.2 Travel data**

532 Travel movement rates were derived from domestic air traffic network data from the U.S. Bureau
533 of Transportation Statistics from January to March 2005 (to represent baseline winter travel in the
534 U.S.). The T100D Market Carriers table had data on the origin metropolitan area, the destination
535 metropolitan area, and the average number of passengers traveling in a given month [61]. The average
536 number of monthly passengers traveling between two metro areas i and j (in either direction),
537 reported in the raw transportation data, was converted to the daily number of passengers w_{ij}
538 traveling between two metro areas and used to determine travel flows between metro areas in the
539 model at each time step. Travel rates were calculated separately for each age group and metro area
540 pair i and j , by considering the population size and age breakdown of metro area i , the daily number
541 of travelers between i and j w_{ij} , and the fraction of children who are travelers r . Children did not
542 travel in the baseline model ($r = 0$), similar to previous studies [4, 33], because only 3% of travelers
543 are children and less than 1% of trips made by children are greater than 30 miles during school term
544 time [20].

545 **S2.3 Holiday intervention period**

546 The holiday period was chosen relative to the epidemic peak in the baseline model, based on the
547 average duration from Christmas to the epidemic peak in the empirical data. The 14-day holiday
548 period began 7 days before Christmas, and ended 7 days after Christmas to reflect the typical length
549 of a winter break school holiday.

550 S2.4 Comparison of baseline and holiday air travel networks

551 We compared the baseline and holiday travel networks across common network measures for un-
552 weighted and weighted networks (Table S2). The baseline network represented average travel pat-
553 terns from January to March 2005 (a typical winter period), the holiday network represented average
554 travel patterns during December 2005 (a typical winter holiday period), and weights represented the
555 average number of monthly passengers between two metro areas. The descriptive characteristics and
556 unweighted network measures present the overall features and potential for connectivity, while the
557 weighted network measures recast connectivity potential in the context of the volume of travel. The
558 baseline network had a greater number of edges and larger average number of absolute connections
559 (unweighted mean degree), while the holiday network had a greater maximum average number of
560 passengers and larger passenger flows (weighted mean degree). This indicates that during the holi-
561 days, there is simultaneously a greater volume of travelers and a lower connectivity potential between
562 airports, perhaps suggesting that this increased volume of holiday travelers seeks out fewer locations
563 (e.g., holiday travelers flock to the largest cities). The holiday network appeared less right-skewed
564 for the unweighted degree distribution and more right-skewed for the weighted degree distribution,
565 corroborating the idea that the baseline network presented greater opportunities for connectivity
566 between airports, but that the holiday network demonstrated an overall greater volume of travel
567 (Figure S4).

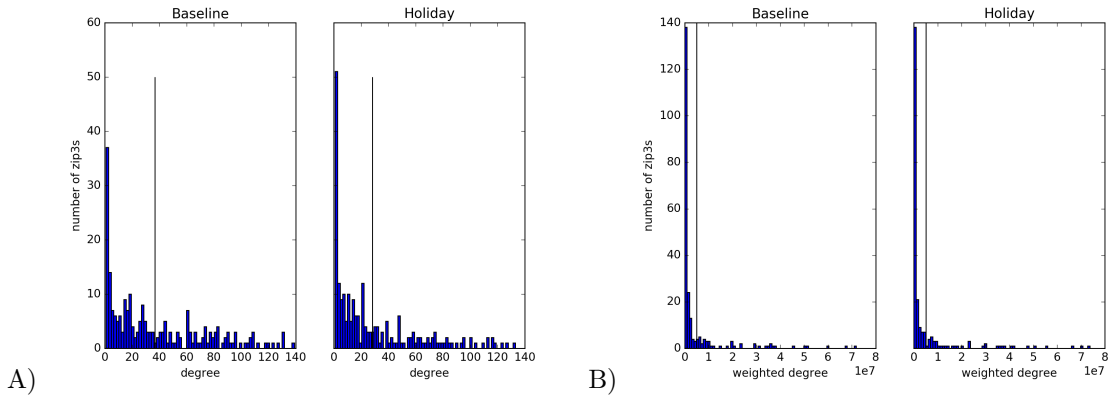
568 These patterns were corroborated in examining differences between holiday and baseline network
569 unweighted and weighted degrees (Figure S5), but differences between urban and rural connectivity
570 during winter baseline and holiday periods may be obscured by the undirected nature of our network
571 edge weights.

572 Airports had many fewer unique airport connections (unweighted degree) during holidays but
573 similar or greater numbers of passengers (weighted degree) flowing through those airports. Notably,
574 in comparing Figure S5A and Figure S5B, all of the decreases in unique airport connections were
575 observed in small and medium sized cities, while airports in populous cities maintained similar
576 numbers of flight connections during the holidays.

Table S2: Comparison of baseline and holiday air travel networks across network measures.

	Baseline	Holiday
Descriptive characteristics		
Number of nodes	228	225
Number of edges	4,189	3,187
Maximum of the average number of monthly passengers between two destinations	7,276,232	7,586,460
Unweighted measures		
Mean degree	36.75	28.33
Transitivity	0.54	0.50
Average clustering coefficient	0.61	0.62
Average shortest path length	2.03	2.11
Weighted measures		
Mean degree	4,904,132	5,106,540
Average clustering coefficient	0.0041	0.0067
Average shortest path length	5,689	14,232

Figure S4: **The holiday air travel network had fewer potential connections and a greater volume of travel than the winter baseline travel network.** A) The unweighted degree distribution appeared more right-skewed for the baseline network, while B) the weighted degree distribution appeared more right-skewed for the holiday network. The black vertical line in each figure represents the unweighted or weighted mean degree, as appropriate.

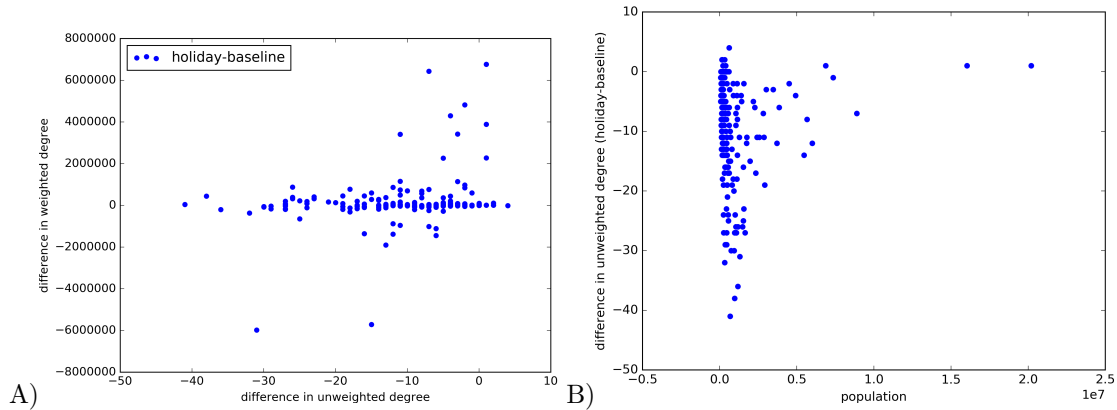


577 S3 Sensitivity Analysis of Model Results

578 S3.1 Contribution of contact reduction vs. assortativity to holiday changes

579 We acknowledge that the contact component of our model’s holiday intervention combines two
 580 changes: 1) an overall reduction in contact rate, and 2) a change in the relative proportion of mixing
 581 between age groups. Here, we compare the baseline and main text contact intervention results
 582 (here, called ‘full school closure’) with simulations that reduced the age-specific number of contacts
 583 but kept assortative mixing among age groups the same as that in the non-holiday contact matrix

Figure S5: **The holiday air travel network experienced increased volume of travelers across similar or fewer unique airport connections.** Baseline network weighted and unweighted degrees were subtracted from holiday network weighted and unweighted degrees to represent the difference in weighted and unweighted degree metrics, respectively. A) Airports tended to have fewer unique connections during the holiday period (difference in unweighted degree) while maintaining similar numbers of passenger throughput (difference in weighted degree). B) In comparing difference in unweighted degree to population, decreases in unique airport connections were observed in small and medium sized cities, while airports in populous cities maintained similar numbers of flight connections during the holidays.



584 ('partial school closure') (Figure S6).

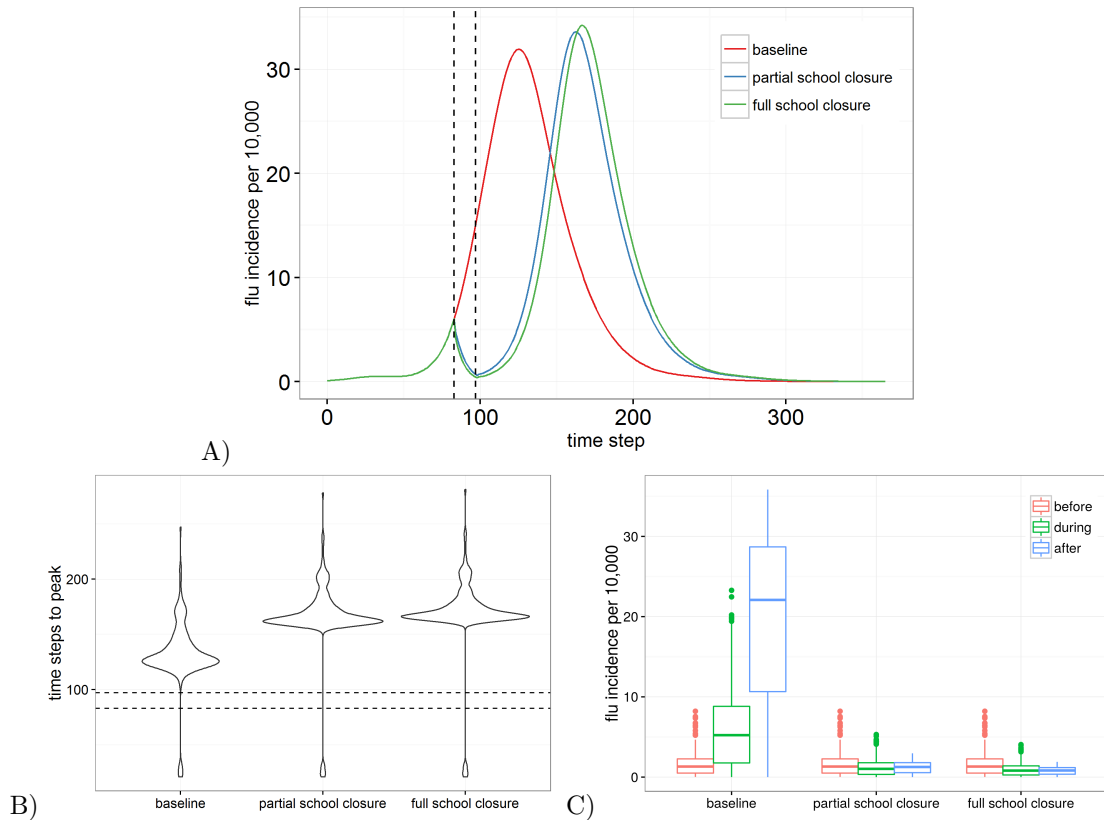
585 S3.2 Sensitivity of epidemic outcomes to contact reduction

586 We examined the sensitivity of epidemic outcomes to overall reductions in contact rate (called 'partial
 587 school closure' in Section S3.1). Two additional sets of simulations were performed, and relative to
 588 the original partial school closure simulations ('partial school closure'), they represented: 1) a 10%
 589 greater reduction in age-specific contacts ('-10% contact rate') and 2) a 10% smaller reduction in
 590 age-specific contacts ('+10% contact rate'). With larger contact rates (+10% contact rate), incidence
 591 peaks were earlier and smaller in magnitude. Synchrony was greater during the holiday period with
 592 lower contact rates than with higher contact rates, as represented with the narrower flu incidence
 593 distribution (Figure S7).

594 S3.3 Sensitivity of epidemic outcomes to holiday timing

595 We examined the sensitivity of model outcomes to holiday timings shifted three weeks ('+3 weeks')
 596 and six weeks ('+6 weeks') forward relative to the holiday timing presented in the main text ('ac-
 597 tual'). The holiday reduced flu incidence to low levels (Figure S8) and shifted relative risk of disease
 598 from children to adults (Figure S9) consistently across various holiday timings. Compared to the
 599 actual holiday simulations, peak timing was delayed for most locations in the +3 weeks simulations,

Figure S6: **A)** Total flu incidence per 10,000 population over time, averaged across all simulations. **B)** Distribution of time steps to peak across all metro areas, averaged across all simulations. **C)** Distributions of flu incidence across all metro areas averaged for the two week durations defined as ‘before’, ‘during’, and ‘after’ the holiday periods, averaged across all simulations. Distributions across metros are compared for the baseline, age-specific reduction in number of contact (partial school closure), and the main text contact only intervention (full school closure) simulations. The intervention period is demarcated by black dashed lines, as appropriate.



600 and only for some locations in the +6 weeks simulations (Figure S10). While we expect holidays to
 601 delay epidemic peaks, many locations had already peaked by the time of the holiday in the +6 weeks
 602 simulations. Similarly, holidays consistently damped flu incidence and increase spatial synchrony
 603 across different timings, but the magnitude of recovery during the ‘after’ holiday period depended
 604 on the remaining susceptibility of the population (Figure S11).

Table S3: Percentage infected out of the total population, averaged across simulations.

Holiday Timing	Baseline	Travel	(Full) School Closure	Partial School Closure	Holiday
No holiday	18.28	-	-	-	-
Actual	-	18.32	17.68	17.67	17.73
+3 weeks	-	18.26	16.02	-	15.96
+6 weeks	-	18.29	14.92	-	14.89

Figure S7: **A)** Total flu incidence per 10,000 population over time, averaged across all simulations. **B)** Distribution of time steps to peak across all metro areas, averaged across all simulations. **C)** Distributions of flu prevalence across all metro areas averaged for the two week durations defined as ‘before’, ‘during’, and ‘after’ the holiday periods, averaged across all simulations. Distributions across metros are compared for partial school closure, and 10% greater reduction (-10% contacts) and 10% smaller reduction (+10% contacts) in age-specific number of contacts. The intervention period is demarcated by black dashed lines, as appropriate.

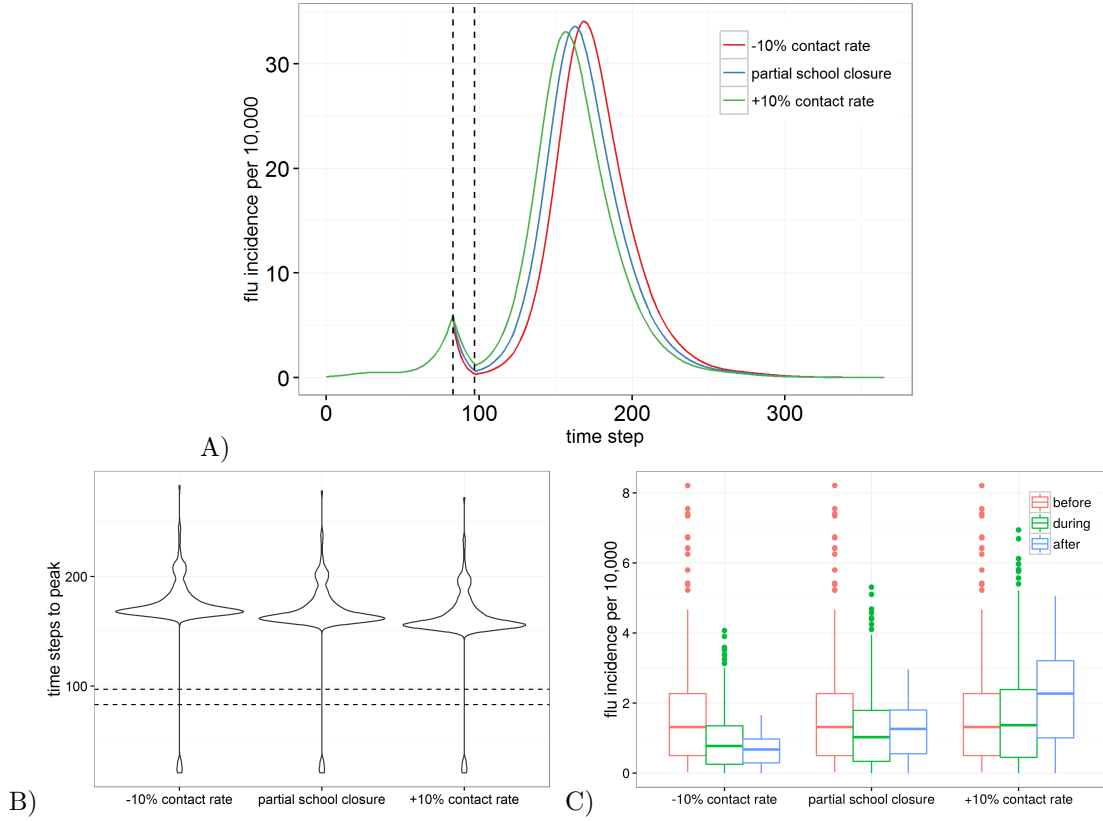


Figure S8: **A)** Total flu incidence per 10,000 population over time, averaged across all simulations for holiday periods shifted forward by **A)** three weeks and **B)** six weeks. Epidemic trajectories for the baseline (no changes during intervention period), travel only, school closure only, and full holiday (travel and school closure changes) interventions are compared, and the intervention period is demarcated by the dashed black lines.

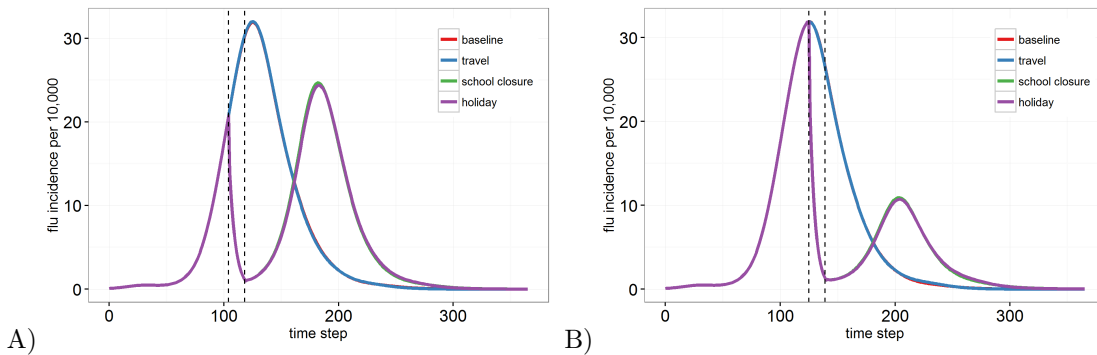


Figure S9: Relative risk of disease from children to adults across all locations, averaged across all simulations, for holiday periods shifted forward by **A)** three weeks and **B)** six weeks. Epidemic trajectories for the baseline (no changes during intervention period), travel only, school closure only, and full holiday (travel and school closure changes) interventions are compared, and the intervention period is demarcated by the dashed black lines.

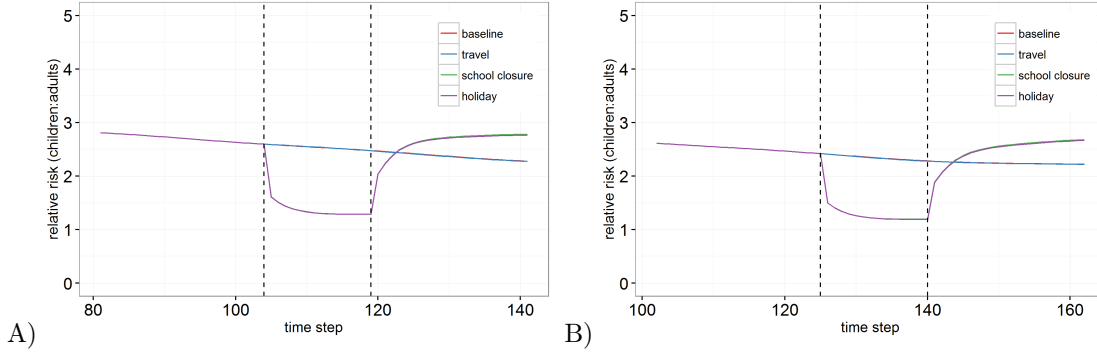


Figure S10: **A)** Distribution of time steps to peak across all metro areas, averaged across all simulations for holiday periods shifted forward by **A)** three weeks and **B)** six weeks. Distributions across metros are compared for the baseline, travel only, school closure only, and full holiday interventions, and the intervention period is demarcated by the dashed black lines.

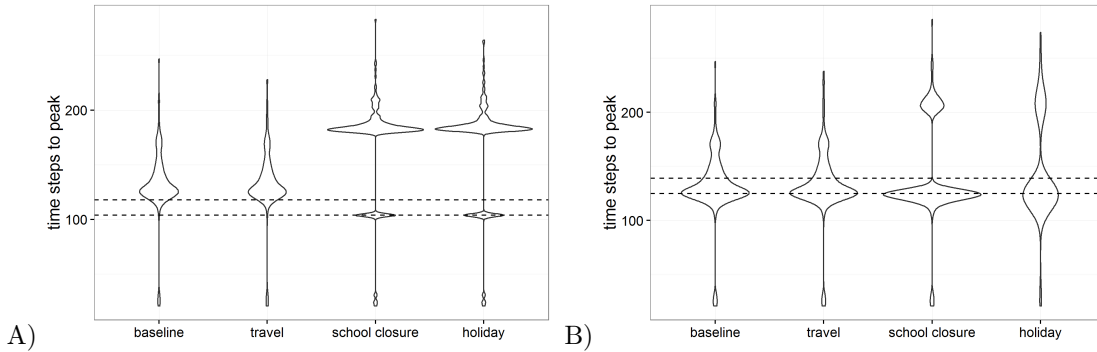
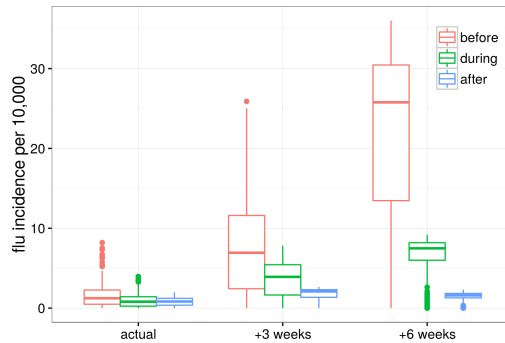


Figure S11: Distributions of flu prevalence across all metro areas averaged for the two week durations defined as ‘before,’ ‘during,’ and ‘after’ the holiday periods for three holiday intervention (travel and school closure) timings, averaged across all simulations.



605 **S3.4 Data access**

606 Simulation code and model outputs averaged across all seeds for all intervention combinations and
607 holiday timings will be made available at <https://github.com/bansallab>.